Graphene Nanoplatelet Cathode for Co(III)/(II) Mediated Dye-Sensitized Solar Cells

Ladislav Kavan,[†,‡,*] Jun-Ho Yum,[‡] Mohammad Khaja Nazeeruddin,[‡] and Michael Grätzel[‡]

[†]J. Heyrovský Institute of Physical Chemistry, v.v.i., Academy of Sciences of the Czech Republic, Dolejškova 3, CZ-18223 Prague 8, Czech Republic, and [‡]Laboratory of Photonics and Interfaces, Institute of Chemical Sciences and Engineering, Swiss Federal Institute of Technology, CH-1015 Lausanne, Switzerland

ABSTRACT Graphene nanoplatelets (GNP) in the form of thin semitransparent film on F-doped SnO_2 (FTO) exhibit high electrocatalytic activity for $Co(L)_2$; where L is 6-(1*H*-pyrazol-1-yl)-2,2′-bipyridine. The exchange current densities for the $Co^{2+/3+}(L)_2$ redox reaction scaled linearly with the GNP film's optical absorbance, and they were by 1−2 orders of magnitude larger than those for the I_3^-/I^- couple on the same electrode. The electrocatalytic activity of GNP films with optical transmission below 88% is outperforming the activity of platinized FTO for the $Co^{2+/3+}(L)_2$ redox reaction. Dye-sensitized solar cells with Y123 dye adsorbed on TiO_2 photoanode achieved energy conversion efficiencies between 8 and 10% for both GNP and Pt-based cathodes. However, the cell with GNP cathode is superior to that with Pt-FTO cathode particularly in fill factors and in the efficiency at higher illumination intensities.

KEYWORDS: graphene · dye sensitized solar cell · cobalt redox shuttle

A dye-sensitized solar cell (DSC) also called a Grätzel cell, represents an attractive alternative to solid state photovoltaics owing to high efficiency, low cost, and ease of fabrication.[1−3] The generic device is a photoelectrochemical DSC, whose key components are dye-sensitized photoanode, electrolyte solution with a redox mediator, and the cathode material. The latter is typically an optically transparent film of Pt nanoparticles on F-doped SnO_2 (Pt-FTO) and the former is the I_3^-/I^- redox couple in aprotic electrolyte medium.

There were several attempts to replace Pt-FTO by other materials such as carbons,[4−13] conducting polymers,[14−16] and others,[5,17−21] but none of the alternative materials was superior to Pt-FTO in terms of optical transparency and electrochemical activity for the I_3^-/I^- redox couple. In general, the quality of a catalytic electrode is characterized by a charge transfer resistance, R_{CT} which scales inversely with the exchange current density, j_o:

$$j_0 = \frac{RT}{nFR_{CT}} \qquad (1)$$

where R is the gas constant, T is temperature, n is the number of electrons, and F is the Faraday constant. Assuming typical photocurrent densities on the TiO_2 photoanode working under full sun illumination[3] to be *ca.* 20 mA/cm^2, eq 1 provides an estimate of R_{CT} of 1.3 Ω cm^2 for the same j_o value on the cathode. Such values are accessible for I_3^-/I^- on a Pt-FTO cathode[4,22,23] as well as on thick (nontransparent) carbon layers.[4,24,25]

Trancik *et al.*[6] stipulated that the carbonaceous film, which would, eventually, replace Pt-FTO for a cathode of DSC should have the following parameters: 80% optical transparency at a wavelength of 550 nm, R_{CT} of 2−3 Ω cm^2 and sheet resistance of 20 Ω/sq. Such a film was not yet demonstrated experimentally. The problem is that the electrocatalytic activity of carbon for the I_3^-/I^- reaction is generally low and is promoted only by defects and oxidic functional groups at the edge of graphite crystal.[6−8] Consequently, defect-free graphene is hardly the suitable material for a DSC-cathode, and power conversion efficiencies as low as *ca.* half of the efficiency of the reference device with Pt-FTO cathode were reported.[10] However, better performance was found for oxygen-functionalized graphene nanosheets[7,8,26,27] or reduced graphene oxide.[28,29] Recently, Kavan *et al.*[7] reported on the promising activity of commercial graphene nanoplatelets. They were used for the fabrication of an optically transparent cathode for the I_3^-/I^--mediated DSCs, but their performance was not competitive compared to that of the usual DSCs with the Pt-FTO cathode.[7]

Recent progress in the field of DSC has been highlighted by replacing the traditional I_3^-/I^- mediator by various organic[30,31] or organometallic[30,32−34] couples with more positive redox potentials than that of I_3^-/I^- (*ca.* 0.35 V *vs* SHE). The obvious motivation

* Address correspondence to kavan@jh-inst.cas.cz.

Received for review September 5, 2011 and accepted October 13, 2011.

Published online October 13, 2011
10.1021/nn203416d

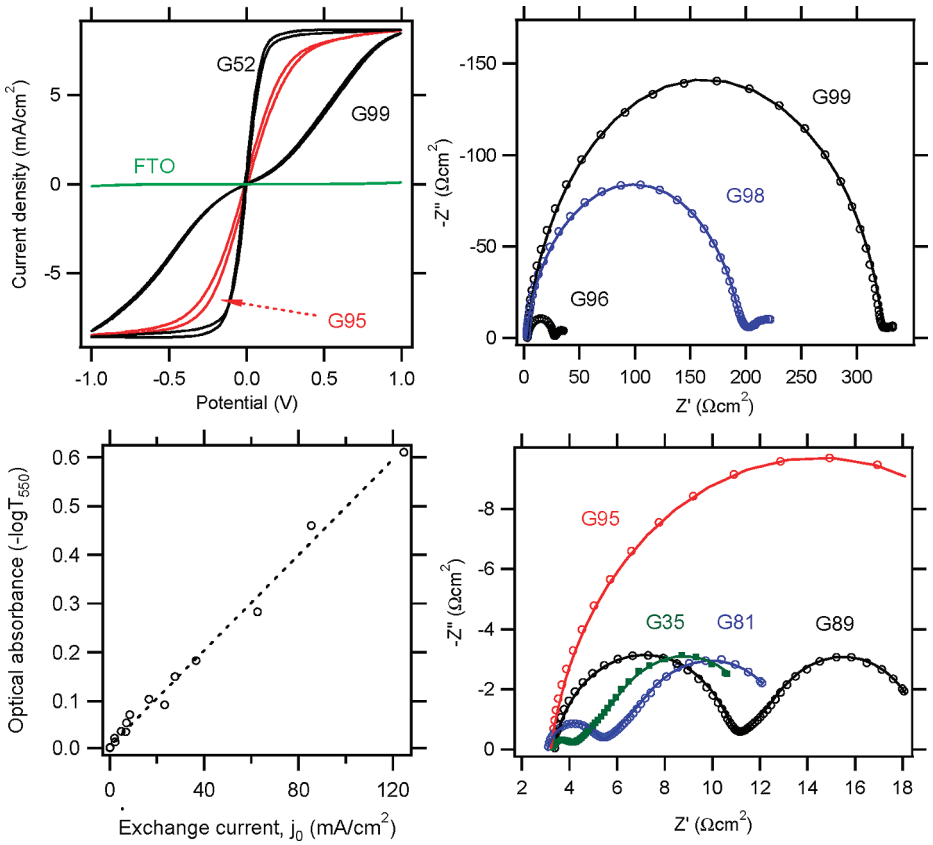

Figure 1. (Left top chart) Cyclic voltammograms of symmetrical dummy cells; scan rate 10 mV/s. (Right top and bottom charts) Nyquist plot of electrochemical impedance spectra measured from 65 kHz to 0.1 Hz on symmetrical dummy cells (bias 0 V). Lines are fitted curves to the equivalent circuit. (Left-bottom) Optical absorbance at a wavelength of 550 nm plotted as a function of exchange current determined from electrochemical impedance spectra.

consists in enhancing the open-circuit voltage of DSC, which would further improve the solar conversion efficiency. Polypyridine complexes of Co(III)/(II) coupled with donor-bridge-acceptor sensitizers, turned out to be particularly promising for this purpose.[33−36] Depending on the polypyridine ligand, the redox potential of Co(III)/Co(II) can be tuned between *ca.* 0.4 and 0.7 V *vs* SHE.[33,37] The corresponding DSCs exhibited open-circuit voltages (V_{oc}) around 0.8−0.9 V which is significantly larger than that of the reference cell with I_3^-/I^- redox shuttle.[33−36] Recently, a novel Co(III)/(II)-complex with tridentate pyridine−pyrazole ligand was introduced as a redox shuttle, rendering V_{oc} over 1 V due to its higher redox potential.[38]

The Co-mediated DSCs[33−35,37,38] employed mostly a Pt-FTO cathode. Recently, Yum *et al.*[38] used nanoporous poly(3,4-propylenedioxythiophene) (PProDOT) showing significant improvement in electrocatalytic activity leading to a higher power conversion efficiency. To the best of our knowledge, there are only two reports on a carbon cathode in conjunction with a Co(III)/(II)-redox mediator.[37,39] Bignozzi *et al.*[37] reported briefly on spray-coated carbon on FTO which worked initially well, even outperforming platinum, but was unstable. Later on, the screen-printed carbon was tested to the same purpose, but its performance was worse than that of platinum.[39] This is somewhat surprising, because Co−polypyridine complexes are known to exhibit faster electron-transfer kinetics on glass-like carbon electrodes compared to that on Pt-electrodes.[37] Here we show that, indeed, Pt-FTO is not necessarily the optimal cathode for Co-mediated DSCs. We report here that the graphene nanoplatelets exhibit excellent activity in this device, outperforming the Pt-FTO in many respects.

RESULTS AND DISCUSSION

The performance of functionalized graphene in Co-(III)/(II)-mediated DSC was evaluated by using the same starting material as in our earlier work,[7] that is, commercial graphene nanoplatelets (GNP), but several upgrades were carried out in the synthetic and characterization techniques (see Experimental Section for details). The used redox shuttle was $Co^{2+/3+}(L)_2$; where L is 6-(1*H*-pyrazol-1-yl)-2,2′-bipyridine (see the chemical formula in Supporting Information Figure S1) in acetonitrile medium. This complex is a particularly promising redox mediator, because it allows the achievement of open-circuit voltages larger than 1 V in dye-sensitized solar cell.[38]

Figure 1 presents electrochemical behavior of symmetrical dummy cells with this electrolyte solution and

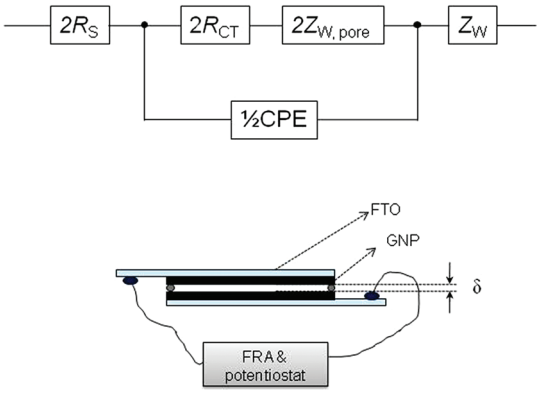

Figure 2. (Top) equivalent circuit diagram for fitting the electrochemical impedance spectra of a dummy cell with two identical electrodes. (Bottom) Scheme of the used cell.

two identical GNP electrodes with graphene nanoplatelets deposited on FTO (see Figure 2 bottom for the cell configuration). The GNP loading on each electrode is labeled arbitrarily as the corresponding optical transmission of the active layer measured at the wavelength of 550 nm, T_{550}. For instance, G95 denotes a sample with T_{550} = 95%, *etc.* (Representative optical spectra are shown in the Supporting Information, Figure S2). The top-left panel in Figure 1 shows cyclic voltammograms of dummy cells with GNP electrodes and also with pure FTO for comparison. The latter material has almost no electrochemical activity at these conditions.

All our voltammograms except for those with very small GNP loading (G99, G98) exhibit a limiting current density of *ca.* 8.5 mA/cm^2, which is controlled by the mass transport in our electrolyte solution. The inverse slope of a voltammogram at the potential of 0 V characterizes the catalytic activity of an electrode; it is, actually, the overall cell resistance (R_{CV}) which can be attained at low current densities.[40] The found R_{CV} values are collected in Table 1.

Electrocatalytic activity of our GNP films is more accurately characterized by electrochemical impedance spectra shown in Figure 1 right panels. The experimental data can be fitted to the equivalent circuit in Figure 2 (top), where R_S is the ohmic serial resistance, $Z_{W,pore}$ is the Nernst diffusion impedance in the pores of carbonaceous material,[8] Z_W is the Nernst diffusion impedance in the bulk electrolyte between electrodes and CPE is constant phase element describing deviation from the ideal capacitance, due to the roughness of the electrodes.[4,22,25,41,42] The corresponding impedance of a constant phase element, Z_{CPE} equals

$$Z_{CPE} = B(i\omega)^{-\beta} \quad (2)$$

where B and β are frequency independent parameters of CPE ($0 \le \beta \le 1$; for $\beta = 1$, the Z_{CPE} transforms into the usual double-layer capacitance).

TABLE 1. Electrochemical Parameters of the Studied Cathode Materials in Symmetrical Dummy Cells

electrode	R_{CV} ($\Omega \cdot cm^2$)	R_s ($\Omega \cdot cm^2$)	R_{CT} ($\Omega \cdot cm^2$)	CPE:B ($S.s^{\beta}$)	CPE: β
FTO-pure	~50 000[a]		~50 000[a]	8×10^{-6}[a]	0.9[a]
G99	350	1.9	158	4.4×10^{-6}	0.95
G98	200	1.5	95	9.4×10^{-6}	0.93
G96	40	1.6	13	1.4×10^{-5}	0.92
G95	37	1.7	12	1.1×10^{-5}	0.92
G92	36	1.8	5	2.0×10^{-5}	0.90
G89	30	1.7	3.7	2.2×10^{-5}	0.90
G88	20	1.6	3.6	2.2×10^{-5}	0.90
G85	18	1.5	3.0	2.4×10^{-5}	0.90
G84	18	1.5	2.8	3.4×10^{-5}	0.90
G83	16	1.6	1.5	4.6×10^{-5}	0.89
G81	16	1.6	1.1	9.4×10^{-5}	0.86
G66	15	1.7	0.70	1.2×10^{-4}	0.86
G52	14	1.6	0.41	2.0×10^{-4}	0.86
G35	12	2[a]	0.3[a]	1×10^{-3}[a]	0.9[a]
G24	12	2[a]	0.2[a]	1×10^{-3}[a]	0.9[a]

[a] Approximate values due to inaccurate fitting of experimental data.

The parameter $Z_{W,pore}$ was introduced by Roy-Mayhew *et al.*[8] for electrodes made from functionalized graphene sheets in contact with I_3^-/I^- electrolyte solution. This additional impedance manifests itself as a third semicircle, which shows up in the high-frequency region of the spectrum measured at applied bias. The parameter $Z_{W,pore}$ can be omitted for Pt-FTO where the catalytic reaction occurs on virtually nonporous surface.[8,22] Also in our case, the diffusion in pores can, obviously, be neglected, because the amount of GNP is too small to create a porous layer on top of FTO. The validity of this assumption is documented by the absence of a third semicircle in the impedance spectra at any bias voltage (*cf.* Supporting Information, Figure S3). Furthermore, the fitted R_{CT} values increased monotonically with bias (Figure S3) which is another principal difference between our GNP|Co(III)/(II) interface and graphene|I_3^-/I^- interface[8] and also the Pt-FTO|-I_3^-/I^- interface[22]).

All our impedance spectra (Figure 1) exhibit just two separated semicircles, which allow simple decoupling of R_{CT} in the high-frequency domain and Z_W in the low frequency domain. The fitting of experimental data to the equivalent circuit shown in Figure 2 (with $Z_{W,pore}$ omitted) is plotted by solid lines in Figure 1. (Several other examples are shown in Supporting Information S4). The low-frequency semicircle has a similar shape independently of the GNP loading (see, *e.g.*, the plots for G35, G81, and G89 electrodes in Figure 1) which expectedly confirms that ionic diffusion in the electrolyte solution is invariant with electrocatalytic activity of electrodes. At zero bias, fitting of this semicircle to Z_W allows determination of the diffusion coefficient; the corresponding values were found between 2×10^{-6} to 4×10^{-6} cm^2/s for all our cells with GNP electrodes as well as with Pt-FTO electrodes (*cf.* Supporting Information

S4). However, Z_W grows dramatically with applied bias (see Figure S3) which is another concomitant effect of fast interfacial electron transfer at our GNP electrodes.

Our R_{CT} values (Table 1) are considerably better than those for the same GNP electrodes in contact with I_3^-/I^--containing electrolyte solution.[7] Furthermore, there is two-orders of magnitude difference between the R_{CT} values of G99 and pure FTO (Table 1). This could serve as a sensitive analytical tool for trace amounts of graphene on the FTO surface. The GNP loading of the G99 electrode was about 1 μg/cm^2, as estimated from the concentration and amount of the used precursor solution, see Experimental Section and Figure S1. (We may note that single-layer graphene would be theoretically G97.7 in our notation, with *ca.* 0.08 μg/cm^2).

The CPE parameter, B, is roughly proportional to R_{CT} which gives evidence that the electrocatalytic activity is related to the surface area of our graphene nanoplatelets. This further manifests itself as a linear fit between the optical absorbance of our electrodes ($-\log T_{550}$) and the inverse charge transfer resistance, $1/R_{CT}$ as in the case of GNP$|I_3^-/I^-$ interface.[7] Since the exchange current, j_o is proportional to $1/R_{CT}$ (*cf.* eq 1) we can also express this fit in the coordinates of ($-\log T_{550}$) *vs* j_o (Figure 1 left bottom chart). According to Lambert–Beer law, absorbance is proportional to concentration (*cf.* Figure S1). Hence, this confirms simple proportionality between j_o (or $1/R_{CT}$) and the concentration of active sites for both the I_3^-/I^- and Co(III)/(II) redox reactions. However, if we compare our actual data for the GNP|Co(III)/Co(II) interface (Figure 1 left bottom chart) with the corresponding values for the GNP$|I_3^-/I^-$ interface,[7] we note that our exchange currents j_o (or our $1/R_{CT}$ values) for Co(III)/(II) are larger by a factor of about 25 or 160 (depending on the reference electrolyte used) than those of the I_3^-/I^- for the given optical transparency. For instance, our G85–G81 films already meet the criteria of Trancik *et al.*[6] in terms of transparency ($T_{550} \geq 80\%$) and charge transfer resistance ($R_{CT} \leq 3\ \Omega\ cm^2$). However, the film must be FTO-supported which still leaves this target open for further experimental efforts. The low serial resistances, R_s, for small graphene loading (Table 1), are obviously due to the conductive FTO support.

We also tested the electrochemical stability of our graphene films. Figure 3 shows the impedance plots for a freshly assembled cell with the G84 electrodes and those after 2 to 11 days of aging. A similar aging effect was reported also for Pt-FTO$|I_3^-/I^-$ interface[7] and was ascribed to the "poisoning" of platinum.[7,22] However, the aging of GNP in contact to Co(III)/(II) redox electrolyte is slower at comparable conditions. (Note that the Pt-FTO$|I_3^-/I^-$ system increased its R_{CT} by a factor of almost five during eleven days of aging (*cf.* Figure 1 in ref 7). Cyclic voltammograms of our G84 dummy cell (data not shown) exhibited no marked aging-dependent changes of their shapes, and also the limiting currents were identical within the experimental errors.

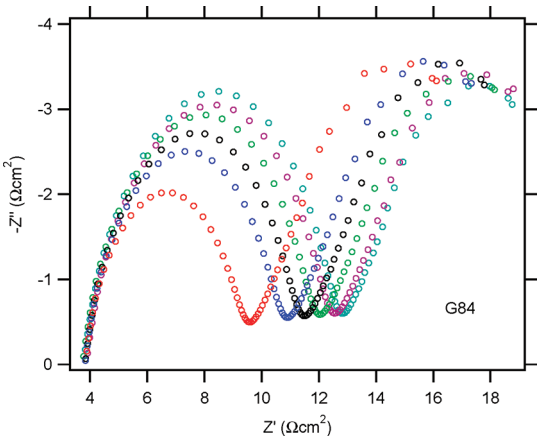

Figure 3. Nyquist plot of electrochemical impedance spectra measured from 65 kHz to 0.1 Hz on symmetrical dummy cell with the G84 electrodes (bias 0 V). Data points were collected for a freshly assembled cell (red) and for that after 2 days (blue), 4 days (black), 7 days (green), 9 days (magenta), and 11 days (cyan) of aging at room temperature.

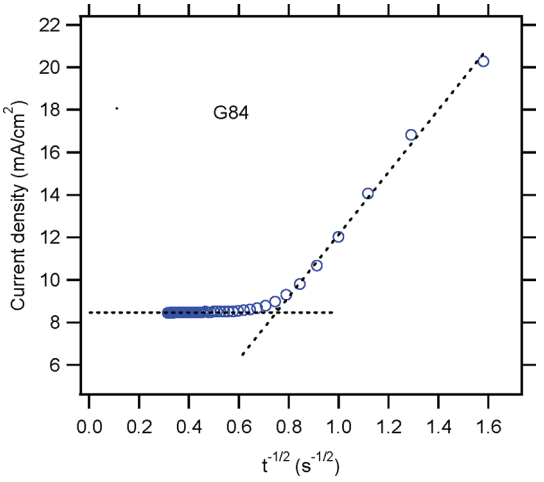

Figure 4. Potential-step chronoamperometry on symmetrical dummy cell with the G84 electrodes. Potential step was from 0 to 0.75 V; time = 10 s.

The electrocatalytic activity of our GNP films with graphene loading exceeding G88 compares favorably to that of the traditional Pt-FTO electrode in the same Co(III)/(II) electrolyte medium. Supporting Information, Figure S4 shows that reference symmetrical dummy cells with Pt-FTO electrodes achieve $R_{CT} = 4.7\ \Omega\ cm^2$ in the freshly assembled state, and there is a similar aging effect as that observed for GNP (*cf.*, Figure 3 and Figure S4).

The occurrence of limiting current plateau on cyclic voltammograms (*cf.*, Figure 1 top left) is typical for Co(III)/(II) redox electrolytes (also on the Pt-FTO electrode, *cf.*, Figure S4 and ref 35), and was not observed for Pt-FTO$|I_3^-/I^-$ interface in methoxypropionitrile medium, the latter exhibiting an almost ideal ohmic behavior between ± 1 V bias.[7] This indicates

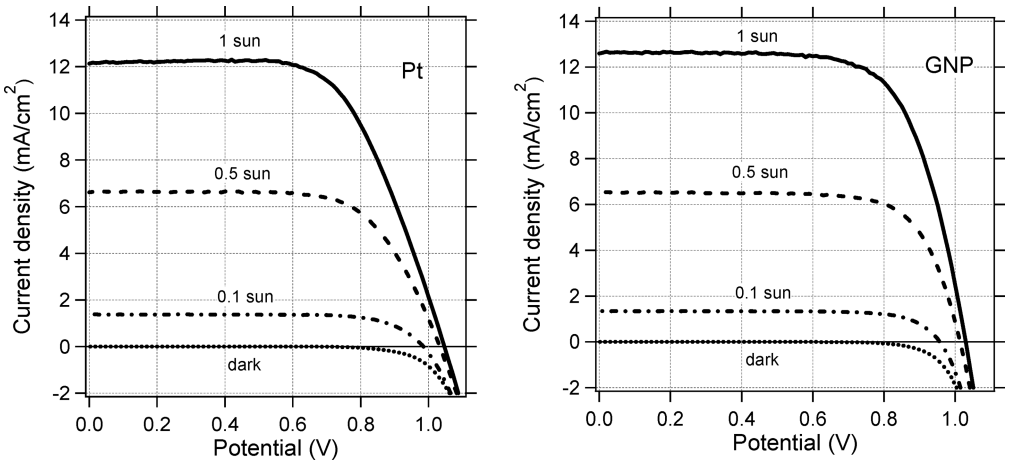

Figure 5. Current–voltage characteristics of dye sensitized solar cells. (Left chart) DSC with Pt-FTO counterelectrode; (right chart) DSC with GNP counterelectrode (G66).

mass-transport limitation of our Co(III)/(II) system. In a symmetrical dummy cell, such effects can be conveniently investigated by potential-step chronoamperometry.[40] Figure 4 shows an example plot for the G84 cell. Shortly after the potential step, the current follows the semi-infinite Cottrell-like decay. The current drops linearly with $t^{-1/2}$ (t is time) as long as the concentration profiles in front of each electrode merge to form a single linear profile. At this stage, the current attains a constant value, similar to the limiting current observed in cyclic voltammograms, ~8.5 mA/cm^2 (*cf.*, Figure 1 top left). Extrapolation of both linear components of the chronoamperometric plot provides intersection at the so-called transition time, τ, which defines the diffusion coefficient, D:

$$D = \frac{\delta^2}{4\pi\tau} \quad (3)$$

(δ is the distance between electrodes, see Figure 2). From the data in Figure 4 and eq 3 we can calculate $D = 2 \times 10^{-6}$ cm^2/s for our system. Obviously, there is a reasonable agreement with values from impedance spectroscopy, see above. In this context, we should note that Wang *et al.*[35] found a limiting current of 39 mA/cm^2 in a dummy cell with Pt-FTO electrodes and $\delta \approx 30$ μm for a similar electrolyte medium, that is, tris(1,10-phenanthroline)Co(III)/(II) in acetonitrile solution (with $D = 7 \times 10^{-6}$ cm^2/s and concentration c = 0.1 mol/L of Co(III)). As the limiting current density, j_L scales linearly with Dc/δ,

$$j_L = 2nFcD/\delta \quad (4)$$

there is a good matching of this limiting current with our value (j_L = 8.5 mA/cm^2) considering the different Dc/δ parameters. Second, our diffusion coefficient is similar to that reported for I_3^-/I^- electrolyte solution in methoxypropionitrile (1.5×10^{-6} to 3.3×10^{-6} cm^2/s) where j_L = 28 mA/cm^2 was achieved due to a larger concentration of I_3^- and, presumably, also a smaller δ value.[43] This leads to an optimistic conclusion that the mass-transport problem in Co-mediated DSC can be addressed successfully.

TABLE 2. Characteristics of Solar Cells with Y123-Sensitized TiO_2 Photoanode and Pt or GNP (G66) Cathodes under Various Light Intensities (I_0)[a]

cathode	I_o (sun)	j_{SC} (mA/cm^2)	V_{OC} (mV)	FF	η (%)
GNP	1	12.7	1030	0.70	9.3
GNP	0.5	6.52	1013	0.73	9.7
GNP	0.1	1.34	956	0.76	9.7
Pt	1	12.1	1047	0.63	8.1
Pt	0.5	6.62	1033	0.68	9.2
Pt	0.1	1.37	984	0.74	10.0

[a] Short circuit photocurrent density = j_{SC}, open-circuit voltage = V_{OC}, fill factor = FF, solar conversion efficiency = η.

Finally, we tested the performance of dye-sensitized solar cells with our GNP cathode and Pt-FTO cathode for comparison. Figure 5 and Table 2 show the corresponding data from current–voltage characteristics under simulated solar irradiation. Even though our DSC devices were not optimized, they demonstrate high power conversion efficiencies between 8 and 10% for both cathode types. The cell with GNP cathode is outperforming that with Pt-FTO particularly in fill factors and in the conversion efficiency at higher illumination intensities. This is an obvious effect of larger electrocatalytic activity (smaller R_{CT}) at the GNP cathode. However, there is also a slight increase of dark current for the GNP-based device, which reduces the efficiency at 0.1 sun and the V_{oc}. In summary, this study confirms that the combination Co–redox–shuttle with a GNP cathode is a promising strategy for further development of dye-sensitized solar cells.

CONCLUSIONS

Graphene nanoplatelets (GNP) deposited in the form of thin semitransparent film on F-doped SnO_2

(FTO) exhibit high electrocatalytic activity for $Co(L)_2$; where L is 6-(1*H*-pyrazol-1-yl)-2,2′-bipyridine. This complex is a promising redox mediator for a novel type of iodine-free dye-sensitized solar cell with open-circuit voltage exceeding 1 V.

Interfacial charge transfer and mass transport in acetonitrile solution of $Co(L)_2$ were characterized by using cyclic voltammetry, potential-step chronoamperometry, and electrochemical impedance spectroscopy on symmetrical thin-layer dummy cells. The exchange current density for the $Co^{2+/3+}(L)_2$ redox reaction scaled linearly with the GNP film's optical absorbance, as in the case of the previously studied I_3^-/I^- redox reaction.[7] However, the exchange currents for $Co^{2+/3+}(L)_2$ couple on the GNP-electrode are larger by a factor of about 25 or 160 than those for the I_3^-/I^- couple on the same electrode (depending on the reference electrolyte used).

The electrocatalytic activity of GNP films with optical transmission below 88% is outperforming the electrocatalytic activity of platinized FTO for the $Co^{2+/3+}(L)_2$ redox reaction. Since Pt-FTO is still the most often used counterelectrode for both for the I_3^-/I^- mediated as well as Co-mediated solar cells, our study asks for revision of this convention for the Co-mediated DSCs.

Dye-sensitized solar cells with Y123+TiO_2 photoanode demonstrate energy conversion efficiencies between 8 and 10% for both GNP and Pt-based cathodes. The cell with GNP cathode is outperforming that with Pt-FTO particularly in fill factors and in the efficiency at higher illumination intensities. This is an obvious effect of smaller R_{CT} at the GNP cathode, but there is also a slight increase of dark current for GNP-based devices, which reduces efficiency at 0.1 sun and the V_{oc}.

EXPERIMENTAL SECTION

Materials. Graphene nanoplatelets, grade 3 (GNP) were purchased from Cheap Tubes, Inc. (USA). According to the manufacturer's specification, they consisted of several sheets of graphene with an overall thickness of approximately 5 nm (ranging from 1 to 15 nm) and particle diameters less than 2 μm and surface area of 600−750 m^2/g. The platelets were dispersed in 2-propanol by sonication (*ca.* 1 min), and the solution was left overnight to separate big particles by sedimentation. The supernatant dispersion containing about 1.2 mg/mL was stable for several days without marked sedimentation. FTO glass (TEC 15 from Libbey-Owens-Ford, 15 Ohm/sq) was ultrasonically cleaned in isopropyl alcohol followed by a 30 min treatment in a UVO-Cleaner (model 256-220, Jelight Co., Inc.). The stock GNP dispersion, which was sometimes diluted to concentrations 0.6 mg/L and 0.3 mg/mL, was then drop-casted on the cleaned FTO. A uniform semitransparent film was obtained after drying at room temperature. The amount of deposited graphene was adjusted by concentration of the used dispersion and/or by repeating the drop casting deposition. The film was finally annealed in Ar atmosphere at 500 °C for 1 h. Platinized FTO was prepared by deposition of *ca.* 5 $\mu L/cm^2$ of 10 mM H_2PtCl_6 in 2-propanol and calcination at 400 °C for 15 min.[4,44]

The symmetrical sandwich dummy cell was fabricated from two identical FTO sheets which were separated by 70 μm thick Surlyn (Solaronix, Switzerland) tape as a seal and spacer leaving 0.6 × 0.6 cm^2 active area. The sheet edges were coated by ultrasonic soldering (Cerasolzer alloy 246, MBR Electronics GmbH) to improve electrical contacts. The distance between electrodes was measured by a digital micrometer, and the average value was 61 ± 5 μm. To present comparable electrochemical data, avoiding small sample-to-sample variations in cell thicknesses, the measured current densities were corrected by a coefficient of $61/\delta_G$, where δ_G is the measured thickness of the actual dummy cell. The cell was filled with an electrolyte through a hole in one FTO support and was finally closed by a Surlyn seal. The electrolyte solution was 0.22 M $Co(L)_2(PF_6)_2$, 0.05 M $Co(L)_2(PF_6)_3$, 0.1 M $LiClO_4$, and 0.2 M 4-*tert*-butylpyridine in acetonitrile; L is 6-(1*H*-pyrazol-1-yl)-2,2′-bipyridine.

Photoelectrochemical tests, were carried out with TiO_2 films with a "double layer" architecture: The transparent layer (thickness, 4.5 μm) was composed of nanocrystalline anatase of ∼20 nm particle size which was deposited on top of $TiCl_4$-treated FTO. The scattering layer (thickness, 4.2 μm) was from 400 nm sized particles (CCIC, HPW-400) and the final film was again treated with $TiCl_4$. The TiO_2 electrode was sensitized with 3[6-[4-[bis(2′,4′-dihexyloxybiphenyl-4-yl)amino-]phenyl]-4,4-dihexyl-cyclopenta-[2,1-b:3,4-b']dithiophene-2-yl]-2-cyanoacrylic acid, coded Y123 by overnight dipping. Details about photoanode fabrication are described elsewhere.[34,38] The DSC was assembled with a counterelectrode using a Surlyn tape (25 μm in thickness) as a seal and spacer (see above). The cell active area for illumination was 0.2 cm^2, defined by a mask.

Methods. Electrochemical measurements were carried out using the PAR 273 potentiostat (EG&G) interfaced to a Solartron 1260A frequency response analyzer and controlled by CorrWare program. Electrochemical impedance data were processed using Zplot/Zview software. The impedance spectra were acquired in the frequency range from 65 kHz to 0.1 Hz, at 0 V bias voltage; the modulation amplitude was 10 mV. The optical spectra were measured by Varian Cary 5 spectrometer with integrating sphere in transmission mode. A blank FTO sheet served as a reference. Hence, all our optical spectra (and the transmittance values quoted in the text for each particular electrode) are normalized by subtracting the absorbance of the FTO support. For photoelectrochemical tests, the light source was a 450 W xenon light source (Osram XBO 450, Germany) with a filter (Schott 113). The light power was regulated to the AM 1.5G solar standard by using a reference Si photodiode equipped with a color-matched filter (KG-3, Schott) to reduce the mismatch in the region of 350−750 nm between the simulated light and AM 1.5G to less than 4%. The differing intensities were regulated with neutral wire mesh attenuator. The applied potential and cell current were measured using a Keithley model 2400 digital source meter.

Acknowledgment. This work was supported by the Czech Ministry of Education, Youth and Sports (Contract No. LC-510), by the Academy of Sciences of the Czech Republic (Contracts IAA 400400804 and KAN 200100801), by the FP7-Energy-2010-FET project Molesol (Contract No. 256617). Partial support of this work by NEC Corporation, Japan, is also acknowledged. M.G. is very grateful to the European Research Council (ERC) for supporting of his research under the ERC-2009-AdG Grant No. 247404 MESOLIGHT. M.K.N. and J.H.Y. acknowledge the support from the Korea Foundation for International Cooperation of Science & Technology through the Global Research Lab and WCU Department of Material Chemistry, Korea University, Chungnam, Korea. The authors also thank Dr. Etienne Baranoff, Dr. Chenyi Yi, and Dr. Florian Kessler for their kind assistance.

Supporting Information Available: Supplemental figures as described in the text. This material is available free of charge *via* the Internet at http://pubs.acs.org.

REFERENCES AND NOTES

1. Grätzel, M. Photoelectrochemical Cells. *Nature* **2001**, *414*, 338–344.
2. O'Regan, B.; Grätzel, M. A Low-Cost High Efficiency Solar Cell Based on Dye-Sensitized Titanium Dioxide. *Nature* **1991**, *353*, 737–740.
3. Hagfeldt, A.; Boschloo, G.; Sun, L.; Kloo, L.; Pettersson, H. Dye-Sensitized Solar Cells. *Chem. Rev.* **2010**, *110*, 6595–6663.
4. Murakami, T. N.; Ito, S.; Wang, Q.; Nazeeruddin, M. K.; Bessho, T.; Cesar, I.; Liska, P.; Humphry-Baker, R.; Comte, P.; Pechy, P.; et al. Highly Efficient Dye Sensitized Solar Cells Based on Carbon Black Counter Electrodes. *J. Electrochem. Soc.* **2006**, *153*, A2255–A2261.
5. Papageorgiou, N. Counter-Electrode Function in Nanocrystalline Photoelectrochemical Cell Configurations. *Coord. Chem. Rev.* **2004**, *248*, 1421–1446.
6. Trancik, J. E.; Barton, S. C.; Hone, J. Transparent and Catalytic Carbon Nanotube Films. *Nano Lett.* **2008**, *8*, 982–987.
7. Kavan, L.; Yum, J. H.; Grätzel, M. Optically Transparent Cathode for Dye-Sensitized Solar Cells Based on Graphene Nanoplatelets. *ACS Nano* **2011**, *5*, 165–172.
8. Roy-Mayhew, J. D.; Bozym, D. J.; Punckt, C.; Aksay, A. Functionalized Graphene as a Catalytic Counter Electrode in Dye-Sensitized Solar Cells. *ACS Nano* **2010**, *10*, 6203–6211.
9. Zhang, Q.; Zhang, Y.; Huang, S.; Huang, X.; Luo, Y.; Meng, Q.; Li, D. Application of Carbon Counterelectrode on CdS Quantum Dot-Sensitized Solar Cells. *Electrochem. Commun.* **2010**, *12*, 327–330.
10. Xu, Y.; Bai, H.; Lu, G.; Li, C.; Shi, G. Flexible Graphene Films *via* the Filtration of Water-Soluble Noncovalent Functionalized Graphene Sheets. *J. Am. Chem. Soc.* **2008**, *130*, 5856–5857.
11. Joshi, P.; Zhang, L.; Chen, Q.; Galipeau, D.; Fong, H.; Qiao, Q. Electrospun Carbon Nanofibers as Low-Cost Counter Electrode for Dye-Sensitized Solar Cells. *ACS Appl. Mater. Interface* **2010**, *2*, 3572–3577.
12. Mei, X.; Cho, J. C.; Fan, B.; Ouyang, J. High-Performance Dye-Sensitized Solar Cells with Gel-Coated Binder-free Carbon Nanotube Films as Counter Electrode. *Nanotechnology* **2010**, *21*, 395202–3952029.
13. Veerappan, G.; Bojan, K.; Rhee, S. W. Sub-micrometer-Sized Graphite as a Conducting and Catalytic Counter Electrode for Dye-Sensitized Solar Cells. *ACS Appl. Mater. Interface* **2011**, *3*, 857–862.
14. Ahmad, S.; Yum, J. H.; Butt, H. J.; Nazeeruddin, M. K.; Grätzel, M. Efficient Platinum-free Counter Electrodes for Dye-Sensitized Solar Cell Applications. *Chemphyschem* **2010**, *11*, 2814–2819.
15. Ahmad, S.; Yum, J. H.; Xianxi, Z.; Grätzel, M.; Butt, H. J.; Nazeeruddin, M. K. Dye-Sensitized Solar Cells Based on Poly(3,4-ethylenedioxythiophene) Counter Electrode Derived from Ionic Liquids. *J. Mater. Chem.* **2010**, *20*, 1654–1658.
16. Tian, H.; Yu, Z.; Hagfeldt, A.; Kloo, L.; Sun, L. Organic Redox Couples and Counter Electrode for Dye-Sensitized Solar Cells. *J. Am. Chem. Soc.* **2011**, *133*, 9422.
17. Jiang, Q. W.; Li, G. R.; Liu, S.; Gao, X. P. Surface-Nitrided Nickel with Bifunctional Structure as Low-Cost Counter-Electrode for Dye Sensitized Solar Cells. *J. Phys. Chem. C* **2010**, *114*, 13397–13401.
18. Wang, M.; Anghel, A. M.; Marsan, B.; Cevey, Ha, N.L.; Pootrakulchote, N.; Zakeeruddin, S. M.; Grätzel, M. CoS Supersedes Pt as Efficient Electrocatalyst for Triiodide Reduction in Dye Sensitized Solar Cells. *J. Am. Chem. Soc.* **2009**, *131*, 15976–15977.
19. Murakami, T. N.; Grätzel, M. Counter Electrodes for DSC: Application of Functional Materials as Catalysts. *Inorg. Chim. Acta* **2008**, *361*, 572–580.
20. Hong, W.; Xu, Y.; Lu, G.; Li, C.; Shi, G. Transparent Graphene/PEDOT-PSS Composite Films as Counter Electrodes of Dye-Sensitized Solar Cells. *Electrochem. Commun.* **2008**, *10*, 1555–1558.
21. Wu, M.; Lin, X.; Hagfeldt, A.; Ma, T. Low-Cost Molybdenum Carbide and Tungsten Carbide Counter Electrodes for Dye-Sensitized Solar Cells. *Angew. Chem., Int. Ed.* **2011**, *50*, 3520–3524.
22. Hauch, A.; Georg, A. Diffusion in the Electrolyte and Charge-Transfer Reaction at the Platinum Electrode in Dye Sensitized Solar Cells. *Electrochim. Acta* **2001**, *46*, 3457–3466.
23. Chen, C. M.; Chen, C. H.; Wei, T. C. Chemical Deposition of Platinum on Metallic Sheets as Counterelectrodes for Dye-Sensitized Solar Cells. *Electrochim. Acta* **2010**, *55*, 1687–1695.
24. Ramasamy, E.; Lee, W. J.; Lee, D. Y.; Song, J. S. Nanocarbon Counterelectrode for Dye Sensitized Solar Cells. *Appl. Phys. Lett.* **2007**, *90*, 173103–1731033.
25. Wang, G.; Xing, W.; Zhou, S. Application of Mesoporous Carbon to Counter Electrode for Dye Sensitized Solar Cells. *J. Power Sources* **2009**, *194*, 568–573.
26. Hsieh, C. T.; Yang, B. H.; Lin, J. Y. One- and Two-Dimensional Carbon Nanomaterials as Counter Electrodes for Dye-Sensitized Solar Cells. *Carbon* **2011**, *49*, 3092–3097.
27. Choi, H.; Kim, H.; Hwang, S.; Choi, W.; Jeon, M. Dye Sensitized Solar Cells Using Graphene-Based Carbon Nano Composite as Counter Electrode. *Solar Energy Mater. Sol. Cells* **2010**, *95*, 323–325.
28. Choi, H.; Kim, H.; Hwang, S.; Han, Y.; Jeon, M. Graphene Counterelectrode for Dye-Sensitized Solar Cells. *J. Mater. Chem.* **2011**, *21*, 7548–7551.
29. Wan, L.; Wang, S.; Wang, X.; Dong, B.; Xu, Z.; Zhang, X.; Bing, Y.; Peng, S.; Wang, J.; Xu, C. Room-Temperature Fabrication of Graphene Films on Variable Substrates and Its Use as a Counter Electrodes for Dye-Sensitized Solar Cells. *Solid State Sci.* **2011**, *13*, 468–475.
30. Hamann, T. W.; Ondersma, J. W. Dye-Sensitized Solar Cell Redox Shuttles. *Energy Environ. Sci.* **2011**, *4*, 370–381.
31. Wang, M.; Chamberland, N.; Breau, L.; Moser, J.; Humphry-Baker, R.; Marsan, B.; Zakeeruddin, S. M.; Grätzel, M. An Organic Redox Electrolyte to Rival Triiodide/Iodide in Dye-Sensitized Solar Cells. *Nat. Chem.* **2010**, *2*, 385–389.
32. Daeneke, T.; Kwon, T. H.; Holmes, A. B.; Duffy, N. W.; Bach, U.; Spiccia, L. High-Efficiency Dye-Sensitized Solar Cells with Ferrocene-Based Electrolytes. *Nat. Chem.* **2011**, *3*, 211–215.
33. Feldt, S. M.; Gibson, E. A.; Gabrielsson, E.; Sun, L.; Boschloo, G.; Hagfeldt, A. Design of Organic Dyes and Co Polypyridine Redox Mediators. *J. Am. Chem. Soc.* **2010**, *132*, 16714–16724.
34. Tsao, H. N.; Yi, C.; Moehl, T.; Yum, J. H.; Zakeeruddin, S. M.; Nazeeruddin, M. K.; Grätzel, M. Cyclopentadithiophene Bridged Donor-Acceptor Dyes Achieve High Power Conversion Efficiencies in Dye-Sensitized Solar Cells Based on Tris-Cobalt-Bipyridine Redox Couple. *ChemSusChem* **2011**, *4*, 591–594.
35. Zhou, D.; Yu, Q.; Cai, N.; Bai, Y.; Wang, Y.; Wang, P. Efficient Organic Dye-Sensitized Thin-Film Solar Cells Based on the Tris(1,10-phenanotroline)Cobalt(II/III) Redox Shuttle. *Energy Environ. Sci.* **2011**, *4*, 2030–2034.
36. Liu, J.; Zhang, J.; Xu, M.; Zhou, D.; Jing, X.; Wang, P. Mesoscopic Titania Solar Cells with Tris(1,10-phenanthroline)cobalt Redox Shuttle. *Energy Environ. Sci.* **2011**, *4*, 3021–3029.
37. Sapp, S. A.; Elliot, M.; Contado, C.; Caramori, S.; Bignozzi, C. A. Substituted Polypyridine Complexes of Cobalt(II/III) as Efficient Electron-Transfer Mediators in Dye-Sensitized Solar Cells. *J. Am. Chem. Soc.* **2002**, *124*, 11215–11222.
38. Yum, J. H.; Baranoff, E.; Kessler, F.; Moehl, T.; Ahmad, S.; Bessho, T.; Marchioro, A.; Ghadiri, E.; Moser, J. E.; Nazeeruddin, M. K.; et al. . Rationally Designed Cobalt Complexes as Redox Shuttle for Dye-Sensitized Solar Cells to Exceed 1000 mV. *Nat. Commun.* **2011**,
39. Ghamouss, F.; Pitson, R.; Odobel, F.; Boujtita, M.; Caramori, S.; Bignozzi, C. A. Characterization of Screen Printed Carbon Counterelectrodes for Co(II)/(III) Mediated Photoelectrochemical Cells. *Electrochim. Acta* **2010**, *55*, 6517–6522.

40. Liberatore, M.; Petrocco, A.; Caprioli, F.; La Mesa, C.; Decker, F.; Bignozzi, C. A. Mass Transport and Charge Transfer Rates for Co Redox Couple in a Thin-Layer Cell. *Electrochim. Acta* **2010**, *55*, 4025–4029.
41. Liberatore, M.; Decker, F.; Burtone, L.; Zardetto, V.; Brown, T. M.; Reale, A.; Di Carlo, A. Using EIS for Diagnosis of Dye-Sensitized Solar Cells Performance. *J. Appl. Electrochem.* **2009**, *39*, 2291–2295.
42. Li, G.; Wang, F.; Jiang, Q.; Gao, X.; Shen, P. Carbon Nanotubes with Titanium Nitride as Low-Cost Counter Electrode for Dye Sensitized Solar Cells. *Angew. Chem., Int. Ed.* **2010**, *49*, 3653–3658.
43. Wang, Q.; Zhang, Z.; Zakeeruddin, S. M.; Grätzel, M. Enhancement of the Performance of Dye-Sensitized Solar Cell by Formation of Shallow Transport Levels under Visible Light Illumination. *J. Phys. Chem. C* **2008**, *112*, 7084–7092.
44. Papageorgiou, N.; Maier, W. E.; Grätzel, M. An Iodine/Triiodide Reduction Electrocatalyst for Aqueous and Organic Media. *J. Electrochem. Soc.* **1997**, *144*, 876–884.